P-ISSN 2586-9000
E-ISSN 2586-9027
Homepage : https://tci-thaijo.org/index.php/SciTechAsia
Science & Technology Asia
Vol.29 No.1 January - March 2024
Page: [57-81]
Original research article

Application of Fly Ash to Improve Workability, Heat Generation, Autogenous Shrinkage, and Cost-Effectiveness of High Strength Concrete

An Pham-Hoai[1,*], Parnthep Julnipitawong[2], Somnuk Tangtermsirikul[1], Yusuke Ishii[3]

[1]*School of Civil Engineering and Technology, Sirindhorn International Institute of Technology, Thammasat University, Pathum Thani 12120, Thailand*
[2]*Construction and Maintenance Technology Research Center, Sirindhorn International Institute of Technology, Thammasat University, Pathum Thani 12120, Thailand*
[3]*Central Research Laboratory, Taiheiyo Cement Corporation, Japan*

Received 3 October 2023; Received in revised form 21 February 2024
Accepted 4 March 2024; Available online 31 March 2024

ABSTRACT

This study aims to evaluate the full potential of using FA in high strength concrete (HSC) mixtures for relieving the troublesomeness in use of HSC by comparing HSC containing FA with HSC containing silica fume (SF) only and ternary binder HSC containing SF and ground granulated blast furnace slag (GGBS) based on equivalent high strength of 83 MPa and high slump flow of 650mm. In the study, workability, compressive strength, autogenous shrinkage, temperature rise, chloride penetration, and carbonation resistance were tested on nine HSC mixtures with and without FA. Test results reveal that using FA in HSC mixtures reduces their viscosity, particularly in the ternary binder mixtures containing 20% FA and 10% SF. Combining 20% FA with 7% SF in the HSC reduces the maximum temperature measured by the semi-adiabatic temperature rise test. The maximum temperature is equivalent to the HSC mixture with 20% FA or mixture with 30% GGBS and 7% SF in combination. Ternary binder concrete mixtures comprising 20% FA and SF show slightly lower 28-day compressive strength than the SF-only mixtures, but their 91-day compressive strength values are equivalent to those of the SF-only mixtures. Due to the improved microstructures, all HSC mixtures perform well in carbonation and rapid chloride permeability, particularly the ternary binders. In the ternary binder HSC mixtures, although 30% GGBS performs better than 20% FA in terms of compressive strength, utilizing FA in HSC improves concrete performances in terms of viscosity, autogenous shrinkage, heat generation, and rapid chloride permeability as well as cost-effectiveness.

***Corresponding author:** parnthep@siit.tu.ac.th

Keywords: Compressive strength; Durability; Fly ash; Ground granulated blast-furnace slag; High strength concrete; Silica fume

1. Introduction

Currently, the use of high-strength concrete (HSC) has been increasing, and HSC has been playing an important role in the global development of concrete technology for many construction applications. High-rise buildings and superstructures, such as long-span bridges and highway bridges, are commonly constructed with HSC mixtures [1]. In 2005, a concrete mixture with a 28-day compressive strength greater than 55MPa was described as HSC by ACI - 363R [2]. However, HSC has been recently defined as concrete having a compressive strength greater than 12,000psi (83MPa). When HSC mixtures are produced using a high amount of cement and SP dosage, it is much more expensive than normal strength concrete [3, 4]. In HSC mixtures, low w/b ratios are used. As a result, high SP dosages are required, and the concrete viscosity increases. Furthermore, an increase in cement content increases the risk of thermal cracking in the concrete due to heat release during hydration and increases autogenous shrinkage, which adversely influences the durability of concrete for long-life services. Furthermore, cement usage has climbed dramatically, reaching a billion tons per year [5]. The production of Portland cement increases CO_2 emissions by about 5 - 8% of global carbon emissions, having a substantial impact on the environment in terms of greenhouse gas emissions [6, 7].

The use of supplementary cementitious materials (SCMs) such as silica fume (SF), ground granulated blast furnace slag (GGBS), and fly ash (FA) aims not only to relieve environmental impacts caused by excessive consumption of Portland cement but also to improve concrete properties [8, 9]. SF, a well-known highly reactive pozzolanic material, can indispensably ensure high strength at an early age. This is because SF can fill voids among cement particles to achieve higher packing density due to its very fine particles [10]. With a very high specific surface area of 15-30m^2/g [11] and higher than 80% amorphous grassy sphere of silicon dioxide (SiO_2), SF can highly and quickly react with $Ca(OH)_2$, resulting in well-crystallized C-S-H gel [12]. However, the optimum usage of SF in HSC still requires examination. The optimum SF replacement percentage for compressive strength at 28 days was discovered to be varied for each w/b ratio [13]. To incorporate SF in concrete mixtures, Mala et al. [14] indicated that the compressive strength could be enhanced over 80MPa with the use of 7% or 10% SF as a cement replacement. Johari et al. [15] revealed that the compressive strengths of concrete mixtures containing 5%, 10%, and 15% SF were higher than Portland cement only mixtures and mixtures with the combination of other pozzolanic materials such as metakaolin, GGBS, and FA. In the case of HSC mixtures having a very low w/b ratio, SF could not be used to replace cement at the replacement higher than 20% because the mixtures will need high SP dosage, have low workability, high autogenous shrinkage, and high costs [14, 15].

The influences of GGBS on concrete properties have been investigated, with promising results found in terms of mechanical and microstructure characteristics. GGBS is known to have both hydraulic and pozzolanic properties. However, compared to Portland cement, the rate of reaction is somewhat low after 5 days [16]. GGBS can increase compressive strength in the first stage to form calcium silicate hydrate (C-S-H) due to hydraulic properties. The pozzolanic reaction occurs when other components such as SiO_2 and Al_2O_3 react with calcium hydroxide $Ca(OH)_2$ to generate secondary (C-S-H), which improves the mechanical and microstructure properties in the second stage. The hydration and pozzolanic reactions could be activated related to the existence and properties of GGBS [17].

Fly ash, a by-product of coal combustion, is generated from coal-fired power plants. Depending on the sources and compositions of the coal, the reactive components of FA vary, containing mainly silica (both amorphous and crystalline) and aluminum oxides. These components can react with calcium hydroxide $Ca(OH)_2$ to form secondary products, which enhance the mechanical and microstructure properties. The use of FA in HSC is restricted due to its slow pozzolanic reaction [18, 19]. Following this, the recommendation for the replacement levels around 15% to 25% FA or incorporating ternary binder with high reactive materials such as combining FA with lime [21] or SF [14] may be used in HSC mixtures to obtain high compressive strength [20]. When incorporating FA in HSC mixtures, FA has numerous benefits in terms of other aspects than compressive strength. Yoo et al. [22] revealed that replacing 10% and 20% of Portland cement with FA lowers autogenous shrinkage. When 30% and 40% FA were utilized as a partial cement replacement, the chloride diffusion resistance of concrete was improved [23]. Additionally, various investigations have shown the benefit of using GGBS or FA in concrete mixtures. The use of FA was more effective than GGBS to increase workability. Using GGBS as a cement replacement increases autogenous shrinkage [24], but the use of FA reduces it [22].

As mentioned previously, SF is usually applied in HSC to obtain compressive strength over 12,000 psi (83MPa). However, these HSC mixtures have 3 typical problems, i.e., viscosity, heat generation, and autogenous shrinkage. Replacing Portland cement with FA can improve some properties of HSC mixtures with suitable proportions. In HSC mixtures with a low w/b ratio, the incorporation of FA can be expected to reduce SP dosage while maintaining high workability, leading to a reduction in concrete viscosity. A high total binder content in HSC can produce high heat generation, whereas FA can reduce it. HSC with a low w/b ratio generally undergoes large autogenous shrinkage, while fly ash is an effective SCM for autogenous shrinkage reduction. As mentioned above, FA is expected to offer many beneficial properties to HSC. Therefore, HSC mixtures incorporating FA need to be further studied to clarify the advantages. However, most investigations on HSC mixtures have focused only on the effects of fly ash as cement replacement on separate properties such as workability [15], mechanical properties [14, 25], and some of the durability properties. For instance, Erdem et al. [25] reported that in the case of compressive strength in the range of 66-107 MPa of HSC mixtures with combining (10%, 20%, 30%) FA and (5%, 10%, 15%) SF with a controlled slump of 6cm, ternary binder mixtures deliver higher compressive strength than binary binder mixtures with proper replacement levels. Mala et al. [14] investigated the compressive and split tensile strength of binary and ternary binder HSC mixtures containing (20%, 30%, 40%, and 50%) FA and (7% and 10%) SF with a controlled slump of 10 ± 2cm. Anwar et al. [26] examined the chloride binding capacity with and without carbonation of HSC mixtures containing (15% and 25%) FA and (5% and 10%) SF as cement replacement, having 28-day compressive strength and slump in the ranges of 55-80 MPa and 9-12cm, respectively. However, the studies of HSC mixture having equivalent compressive strength and high slump flow class on the evaluation of viscosity, heat generation, autogenous shrinkage, and cost of HSC mixtures are scarce.

This research focuses on utilizing FA to its full potential in HSC mixtures to solve 3 main problems in the use of HSC. It has been recognized that there are 3 key difficulties in using high strength concrete, i.e., high viscosity, high autogenous shrinkage, and high temperature rise. This research aims to address the benefits of FA on properties of HSC with FA by comparing with HSC containing silica fume only and ternary binder HSC comprising SF and GGBS. The mix proportions of

concrete mixtures were designed based on an optimized aggregate phase with the minimum void content. All tested HSC mixtures were controlled to have a slump flow of 65 ± 1cm and 28-day compressive strength over 12,000psi (83MPa). The experimental programs were prepared to inspect the HSC properties such as viscosity, autogenous shrinkage, semi-adiabatic temperature rise, compressive strength, chloride penetration, and carbonation resistance. In addition, Wet Packing Density (WPD), X-ray Diffraction (XRD), and Mercury Intrusion Porosimetry (MIP) were carried out to describe the mechanisms of the resulting performances. Finally, a cost comparison of all tested mixtures was conducted.

2. Materials and Methods

2.1 Materials and mix proportions

2.1.1 Binders

Four types of raw materials were used in the experiment in this study. Ordinary Portland cement type I (C), according to ASTM C150 [27], Fly ash (FA), Ground granulated blast-furnace slag (GGBS), and Silica fume (SF). Chemical compositions and physical properties of C, FA, GGBS, and SF are given in Table 1. Mineralogical compositions analyzed by XRD analysis of all tested binders are shown in Table 2.

Particle shape and size of Portland cement (C), Blended fly ash cement (FC), ground granulated blast-furnace slag (GGBS), and silica fume (SF), analyzed by Scanning Electron Microscope (SEM), are present in Fig. 1. Particle shapes of C and GGBS are irregular with rough surfaces. The shapes of FA and SF are spherical with smooth surfaces. However, the particle size of SF is much smaller than those of the others. As the blended fly ash cement was used in the test, Fig. 1b. is the SEM image of the blended fly ash cement but not fly ash only. The blending ratio of the fly ash cement is 70:30, cement to fly ash.

2.1.2 Superplasticizer (SP)

A polycarboxylate-based SP, MIGHTY 21WH, was used to obtain a controlled slump flow of 65 ± 1cm. The SP is classified as a type F admixture according to ASTM C494 [28].

2.1.3 Aggregates

Coarse aggregate was crushed limestone with a maximum size of 20mm, and natural river sand was used as the fine aggregate. The coarse aggregate and fine aggregate had specific gravities of 2.78g/cm^3 and 2.58g/cm^3 and absorptions of 0.4% and 1.21%, respectively. The gradations of both aggregates fall within the limits specified by ASTM C33 [29].

2.1.4 Mix proportions

The mixtures of paste, mortar, and concrete with and without FA were prepared. Nine paste mixtures with a controlled w/b of 0.21 were used for the wet packing density (WPD) test. The mortar mixtures with a controlled w/b of 0.21 were used for the Mercury Intrusion Porosimetry (MIP) test. The details of the tested mix proportions are presented in Table 3.

Nine concrete mixtures were investigated in this study. The controlled constant parameters for the comparative study were a w/b ratio of 0.21, a total binder content of 600kg/m^3, and an s/a ratio of 0.44. The s/a ratio of 0.44 was the ratio that gave the minimum void content of the mixtures of the coarse and fine aggregates used in this study. The aggregate phase at minimum void content was expected to provide the HSC with the least required amount of paste in the concrete for a specified slump flow. The mixtures of HSC comprising binders with and without FA were used for the investigation.

Table 1. Chemical compositions and physical properties of C, FA, GGBS, and SF used in the tests.

Properties	C	Supplementary cementitious materials (SCMs)		
		FA	GGBS	SF
	Chemical compositions (% by weight)			
Silicon dioxide, SiO_2	20.71	55.39	32.55	93.81
Aluminum oxide, Al_2O_3	5.72	22.83	13.66	0.24
Iron oxide, Fe_2O_3	3.00	6.4	0.37	0.09
Calcium oxide, CaO	65.01	6.74	42.47	0.58
Magnesium oxide, MgO	1.2	2.1	6.13	0.7
Sulfur oxide, SO_3	2.15	-	2.26	0.37
Loss on ignition, LOI	2.21	1.2	0.21	2.11
	Physical properties			
Blaine's fineness (cm^2/g)	3250	3700	4310	17000
Specific gravity (g/cm^3)	3.16	2.36	2.89	2.25

Table 2. Mineralogical analysis of C, FA, GGBS, SF.

	Raw supplementary cementitious materials (SCMs)			
Phase	C	FA	GGBS	SF
C_3S	59.15	-*	-*	-*
C_2S	14.94	-*	-*	-*
C_3A	8.56	-*	-*	-*
C_4AF	9.32	-*	-*	-*
Free Lime	0.09	0.4	-*	-*
Portlandite	1.46	-*	-*	-*
Periclase	0.39	0.52	-*	-*
Quartz	0.03	8.36	-*	0.48
Aphthitalite	0.23	-*	-*	-*
Gypsum	0.36	-*	-*	-*
Bassanite	1.64	-*	-*	-*
Anhydrite	0.01	-*	1.71	-*
Calcite	3.53	0.93	-*	-*
Dolomite	0.29	-*	-*	-*
Magnetite	-*	0.79	-*	-*
Mullite (S_2A_3)	-*	9.41	-*	-*
Silicon Oxide	-*	-*	-*	0.55
Cristobalite	-*	-*	-*	0.68
Amorphous	-*	79.59	98.29	98.29
Total	100	100	100	100

Note: —*: Not found

The use of SF as an SCM in the HSC mixtures was to ensure the target strength over 12,000psi (83MPa). The SF replacement was controlled to be not higher than 10% to ensure slump flow of 65 ± 1 cm, with an appropriate SP dosage. Thus, two concrete mixtures containing SF only, the concrete mixtures containing 7% SF (OS7) and 10% SF (OS10), were considered as reference mixtures. GGBS was used as a comparative SCM to ensure strength in HSC mixtures in ternary binder systems. However, high replacement of GGBS would reduce early-age compressive strength compared with the reference HSC mixtures due to the reduced proportion of cement for early-age hydration. As a result, GGBS was used at 30% replacement to ensure early-age compressive strength. It could also enhance later-age compressive strength development due to pozzolanic reaction [17]. To use GGBS in HSC mixtures for comparison in this study, two concrete mixtures incorporating both GGBS and SF are the concrete mixture containing 30% GGBS and 7% SF (OG30S7), and the concrete mixture incorporating 30% GGBS and 10% SF (OG30S10).

To ensure compressive strength up to 12,000psi (83MPa), a maximum of 20% FA was used in this study. One binary binder HSC mixture using FA-only was designed to contain 20% FA (OF20). Four ternary binder HSC mixtures incorporating FA and SF were prepared which are a concrete mixture containing 10%FA and 7% SF (OF10S7), a

concrete mixture containing 10% FA and 10% SF (OF10S10), a concrete mixture containing 20% FA and 7% SF (OF20S7), and a concrete mixture containing 20% FA and 10% SF (OF20S10). To achieve a slump flow of 65 ± 1cm, a superplasticizer was used. The details of the tested HSC mix proportions are presented in Table 4.

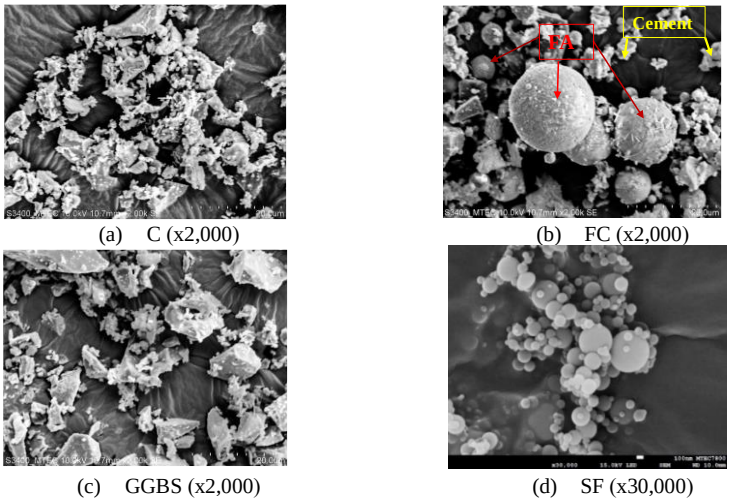

(a) C (x2,000) (b) FC (x2,000)

(c) GGBS (x2,000) (d) SF (x30,000)

Fig. 1. SEM observations of (a) C, (b) FC, (c) GGBS, and (d) SF.

Table 3. Details of test items and mix proportions of the tested pastes and mortars.

Test items	Paste/Mortar	FA	SF	GGBS	w/b ratio
		(% by weight)			
WPD	Paste	10 or 20	7	30	0.21
		10 or 20	10	30	
MIP	Mortar	20	7	30	0.21

Table 4. Details of concrete mix proportions.

Descriptions	Mix ID	SCMs systems FA, GGBS, SF (% by weight)	w/b	Binder (kg/m^3)				Aggregates (kg/m^3)		W (kg/m^3)	SP (kg/m^3)
				C	FC	GGBS	SF	S	G		
No SF	OF20	20% FA	0.21	200	400	-	-	751	1029	126	7.8
7% SF groups	OS7 (Ref.1)	7% SF	0.21	558	-	-	42	759	1041	126	10.92
	OF10S7	10% FA and 7% SF	0.21	358	200	-	42	752	1031	126	10.50
	OF20S7	20% FA and 7% SF	0.21	158	400	-	42	745	1021	126	9.30
	OG30S7	30% GGBS and 7% SF	0.21	378	-	180	42	753	1033	126	10.32
10% SF groups	OS10 (Ref.2)	10%SF	0.21	540	-	-	60	757	1038	126	11.10
	OF10S10	10% FA and 10% SF	0.21	340	200	-	60	749	1028	126	10.8
	OF20S10	20% FA and 10% SF	0.21	140	400	-	60	742	1017	126	9.72
	OG30S10	30% GGBS and 10% SF	0.21	360	-	180	60	751	1029	126	10.62

Note: C – Portland Cement, FC – Blended fly ash cement, SF - Silica fume, GGBS - Ground granulated blast-furnace slag, W - water, S - fine aggregate, G - coarse aggregate, w/b - water to binder ratio, SP - Superplasticizer

2.2 Test methods

In this study, to investigate the applicability of using FA as SCM in HSC, various HSC mixtures were designed. The C-FA binary binder and the C-FA-SF ternary binder systems of HSC mixtures were compared with the binary binder HSC mixtures containing SF only and the ternary binder HSC mixtures containing SF and GGBS.

The experimental programs were divided into 3 stages. In the first stage, the HSC mixtures in Table 4 were mixed with their slump flows adjusted by varying the

superplasticizer dosage to reach the target slump flow. Then, the measurement of T-50cm and V-funnel tests for evaluating the viscosity of the mixtures were conducted. The compressive strength of the HSC mixtures was tested at 7, 28, and 91 days of age. The target compressive strength of concrete mixtures was set at 12,000psi (83MPa) at 28 days in conjunction with a target slump flow of 65 ± 1 cm. In the second stage, autogenous shrinkage, semi-adiabatic temperature rise, carbonation depth, and rapid chloride permeability of the HSC mixtures were investigated. In the third stage, to clarify the influences of FA on the properties of the HSC mixtures, SEM, XRD and Mercury Intrusion Porosimetry were examined by using powder samples and mortar mixtures obtained from the concrete mixtures, respectively. The mix proportions of binders in the tested HSC mixtures were used to prepare paste samples for the WPD test. Finally, WPD, microstructure analyses by SEM, XRD, and MIP are used to clarify the effects of FA on some tested HSC properties.

2.2.1 Wet packing density (WPD)

The wet packing density method, as proposed by Wong et al. [30], was used in this investigation. It was elaborated that using the wet method, the solid volume concentration of the binder's paste is higher than the dry packing density method. The wet condition allows water to lubricate and fill up spaces between particles in the mixtures, resulting in a more accurate measurement of solid volume concentration. Furthermore, the use of SF in the mixtures causes agglomeration, making dry packing density measurements inaccurate [31]. The concept of the method involves the preparation of mixtures with various w/b ratios by volume and measuring the wet density of the paste mixtures. The solid volume concentration obtained from the WPD test can be calculated using Eq. (2.1).

$$\phi = \frac{M/V}{\rho_w u_w + \rho_C R_C + \rho_{FA} R_{FA} + \rho_{GGBS} R_{GGBS} + \rho_{SF} R_{SF}}, \quad (2.1)$$

where M and V are the mass of the paste mixtures and the volume of mold. ρ_w, ρ_C, ρ_{FA}, ρ_{GGBS}, and ρ_{SF} are the specific gravity of water, C, FA, GGBS, and SF, respectively, u_w is the w/b ratio (defined as the ratio of the water volume to the particles solid volume ratio. R_C, R_{FA}, R_{GGBS}, and R_{SF} are the volumetric ratios of C, FA, GGBS, SF, respectively, in the paste mixtures.

2.2.2 Workability

Slump flow was tested according to ASTM C1611 [32]. The T-50_{cm} test was tested according to ASTM C1611 [32]. V-funnel time was tested according to EN 12350-9 [33].

2.2.3 Compressive strength

Three concrete 100x200mm cylinder specimens for each HSC mixture were prepared for compressive strength test according to ASTM C39 [34]. The compressive strength of each concrete mixture was the average of the three specimens. The specimens were tested at 7 days, 28 days, and 91 days of age. All concrete specimens were cured in a water tank until their test ages.

2.2.4 Autogenous shrinkage

Three 75×75×285mm concrete prism samples were prepared for autogenous shrinkage measurement. The length change was measured to examine the autogenous shrinkage of the tested HSC mixtures, according to the ASTM C157 [35]. The tested HSC specimens were sealed with paraffin and many layers of plastic sheets to prevent moisture loss to the environment and were cured in a room at a temperature of 28 ± 2°C and a relative humidity of 75 ± 5%.

2.2.5 Semi-adiabatic temperature rise

The set-up of the semi-adiabatic temperature rise test is shown in Fig. 2. To delay heat loss from the concrete specimens to the air, the semi-adiabatic temperature rise specimens were insulated by 5cm thick polystyrene foams and 1.5cm thick wood

plates. Temperature sensors were installed and measured at the center and the rim (from 5cm on each side) positions of the 40×40×40cm cube specimens. The temperature rise was measured until the temperature was almost constant, approximately at the concrete age of 14 days.

2.2.6 Carbonation depth

Three 100×100×100mm cubic specimens were prepared for the test. The carbonation depths were determined by spraying a solution of 1% phenolphthalein in 70% ethyl alcohol on the freshly broken concrete surfaces. As a result, the phenolphthalein solution turns purple when the pH value is higher than 9. Hence, the carbonation surface is colorless, whereas the non-carbonated surface remains purple, according to RILEM (1998) standards [36].

2.2.7 Rapid chloride permeability test (RCPT)

Three concrete cylinder samples were prepared for the RCP test, according to the ASTM C1202 [37]. The amount of chloride ion passed through the specimens was measured within 6 hours. The tests were conducted on the specimens at the ages of 28 days and 91 days. The chloride permeability was then evaluated according to ASTM C1202, as shown in Table 5.

2.2.8 Microstructure analysis

To investigate the pore structures and the porosity of mortar mixtures, microstructure analysis using Mercury Intrusion Porosimetry (MIP) was performed. The MIP test was used to determine the pore size distribution of the hardened mortar mixtures.

(a)

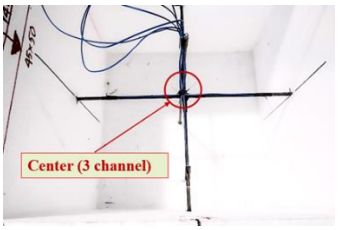

(b)

Fig. 2. Setup experimental program for semi-adiabatic temperature test (a) Laptop, Datalogger, Mold (b) Thermal couple positions.

Table 5. Chloride ion penetration of concrete according to ASTM C1202 [37].

Charge passed (Coulombs)	Chloride ion permeability
< 100	Negligible
100 – 1000	Very low
1000 – 2000	Low
2000 – 4000	Moderate
> 4000	High

3. Results and Discussion

3.1 Solid volume of paste mixtures by WPD test

The results of solid volume concentration tested by the WPD method of binary and ternary binder paste mixtures containing FA, GGBS, and SF are depicted in Fig. 3.

Among all the tested mixtures, the OF20 has the lowest solid volume (0.574), while the OF20S10 mixture has the highest solid volume (0.607). In binary binder combinations, the SF (OS7 and OS10) mixtures have greater solid volumes than the FA (OF20) mixture. Ternary binder systems with FA and SF (OF10S7, OF10S10, OF20S7, and OF20S10), or GGBS and SF (OG30S7, and OG30S10) have higher

solid volumes than the silica fume-only mixtures (OS7 and OS10) when compared at the same SF content.

The differences in physical characteristics of mixtures when incorporating different mineral materials, such as particle shape and texture, particle size distribution, and percentage of blended raw materials, can be used to explain the packing density results [38, 39]. The SF particles in this study are very small and spherical, so they can fill spaces between cement particles well. However, the particle sizes of FA and cement are nearly the same, so when compared to SF, FA is less efficient in filling spaces between cement particles. As a result, for binary binder systems, the two tested SF mixtures (OS7 and OS10) have larger solid volumes than the FA mixture (OF20). In the case of SF ternary binder mixtures containing FA or GGBS, the packing density of FA mixtures is higher than that of GGBS mixtures. Due to the rough surface and irregular shape of GGBS particles, in contrast to the round and smooth-surfaced FA particles depicted in Fig. 1, the mixtures containing the combined SF and FA exhibit superior particle packing compared to those containing the combined SF and GGBS.

3.2 Effects of fly ash on superplasticizer dosage and slump flow performance

The slump flows of the tested HSC mixtures were controlled to be within 65 ± 1cm. Fig. 4 shows the slump flow values of all tested HSC mixtures. The corresponding superplasticizer dosages used to control the slump flow are different for different tested HSC mixtures, as shown in Fig. 5.

To compare the slump flow performance, the slump flow values are normalized by considering superplasticizer dosages (ratio of slump flow to superplasticizer dosage). The ratio is expressed in terms of the ratio of slump flow (SF) to superplasticizer dosage (SP), as shown in Fig. 6. It is noted that normalized SF/SP indicates the effectiveness of SP in the mixtures. The higher normalized SF/SP value means the mixture requires a lower SP dosage to produce the same slump flow. The results show that OF20 has the highest SF/SP value of 8.3, while OS10 concrete mixture has the lowest SF/SP of 5.8. Compared with OS7 and OS10 mixtures, the addition of FA or GGBS in concrete mixtures reduces the dosage of the superplasticizer. The results imply that the addition of FA is beneficial for producing slump flow performance compared to GGBS and SF. Increasing the replacement of FA improves the slump flow performance and increases the efficiency of the superplasticizer. When compared with Portland cement and GGBS, the use of FA reduces water demand [40], while the use of SF increases the water demand of the concrete [41, 42]. Therefore, at a controlled w/b ratio and total binder content, the use of FA reduces the dosage of superplasticizer compared to SF concrete mixtures to produce the same slump flow. The use of SF increases the demand for SP dosage due to its very fine particles (large surface area) and its particle agglomeration. It is noted that although the GGBS reduces the SP dosage of the SF mixtures, it is less effective than the FA.

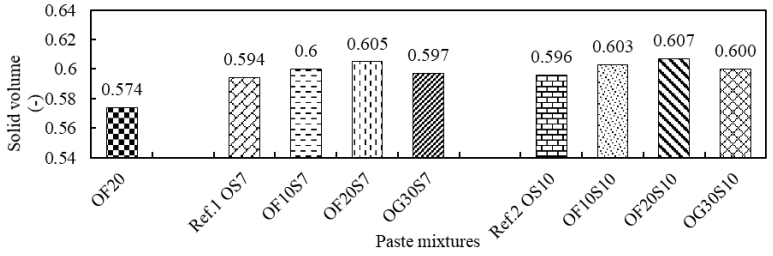

Fig. 3. Effects of binders on solid volume.

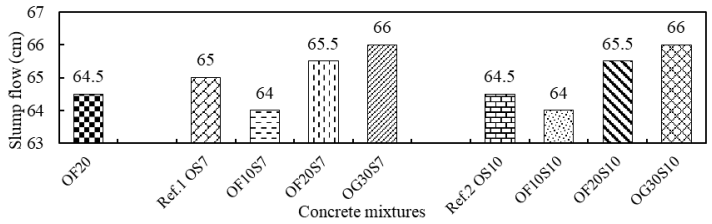

Fig. 4. Slump flow of tested HSC mixtures.

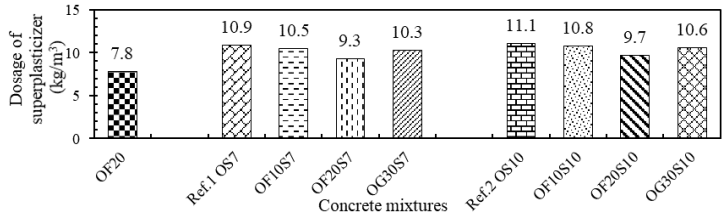

Fig. 5. Dosages of superplasticizer for slump flow control of tested HSC mixtures.

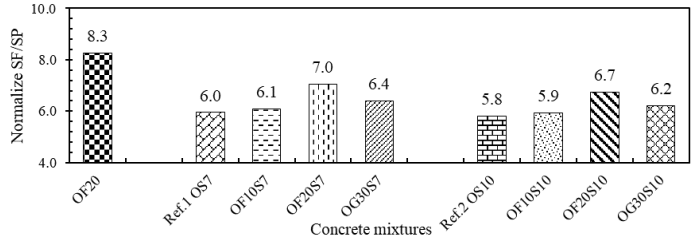

Fig. 6. Normalize slump flow to superplasticizer of the tested concrete mixtures.

3.3 Effects of fly ash on the viscosity of HSC mixtures

To compare the viscosity of different HSC mixtures with and without FA, the slump flow of the HSC mixtures was controlled within 65 ± 1 cm. The T-50_{cm} and V-funnel tests, both are related to the viscosity of HSC mixtures, were conducted, and the results are shown in Figs. 7-8, respectively.

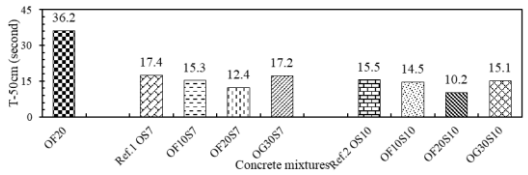

Fig. 7. Results of T-50_{cm} of the tested HSC mixtures.

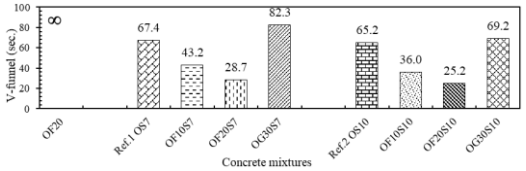

Fig. 8. Results of V-funnel of the tested HSC mixtures.

The T-50_{cm} is closely correlated with the concrete viscosity [43]. When the viscosity of concrete is higher, the T-50_{cm} of the concrete will take longer to reach the slump flow of 50_{cm}. One of the problems in practicing HSC is its high viscosity causing low workability, and so it is difficult to work with during placing, consolidating, and surface finishing. As shown in Fig. 7, compared to the reference concrete mixtures of OS7 and OS10, the binary binder OF20 mixture has the highest T-50_{cm} of 36.2 sec., which is the highest among all the tested mixtures. However, the ternary binder, OF20S10 mixture, has the lowest T-50_{cm} of 10.2 sec. The use of FA is better than GGBS to reduce the viscosity of the HSC mixtures. It can be concluded that the use of FA helps to reduce HSC viscosity more effectively than GGBS, as can be observed by comparing the T-50_{cm} values of OF10S7 and OF20S7 with OG30S7 as well as OF10S10 and OF20S10 with OG30S10.

The results of V-funnel measurement have a close correlation with the deformability and viscosity of flow concrete [43]. The trend of the results of V-funnel time in Fig. 8 is the same as that of the T-50_{cm} in Fig. 7. The binary binder mixture OF20 demonstrates blocking (V-funnel time = ∞) due to high viscosity, while the ternary binder mixture OF20S10 experiences the lowest V-funnel time of 25.2 sec. The viscosity of HSC mixtures containing only SF (OS7 (67.4 sec.)) and OS10 (65.2 sec.)) is significantly higher when compared to ternary binder mixtures with FA. When compared with silica fume binary mixtures OS7 and OS10, the inclusion of FA in the OS7 and OS10 mixtures (OF10S7 (43.2 sec.), OF20S7 (28.7 sec.), OF10S10 (36 sec.), OF20S10 (25.2 sec.)) gives significant improvement in lowering the viscosity by reducing the V-funnel times, while the use of GGBS (OG30S7 (82.3 sec.), OG30S10 (69.2 sec.) increases the V-funnel times of the SF mixtures.

The results of T-50_{cm} and V-funnel corresponding to viscosity properties of the tested HSC mixtures can be explained by 2 main mechanisms (1) packing density and (2) shapes of particles in the tested binary and ternary binder systems [44]. In binary binder systems, the use of SF at 7% or 10% replacement improves the packing density of the SF mixtures compared to the FA mixture as the SF particles are much smaller, and so have better filling ability. When packing density increases, the demand for water to fill voids among particles is reduced, resulting in increased free water for lubrication and flowability of the concrete mixtures, for a constant w/b ratio [45, 46]. In ternary binder systems with SF, FA has a spherical particle shape and smooth surface, whereas GGBS particles are irregular and rough, as shown in Fig. 1. In addition, the ternary binder mixtures with fly ash (OF10S7 and OF10S10) have larger solid volume concentrations than the ternary binder mixtures with GGBS (OG30S7 and OG30S10), respectively. This means that the void contents of the FA ternary binder mixtures are lower than those of the GGBS ternary binder mixtures. Therefore, with the same unit water content, particle distances are larger in the FA ternary binder mixtures, resulting in fewer particle contacts, and so lower resistance to deform. Thus, based on the above explanation, incorporating FA in SF concrete mixtures gives an advantage to reduce the contacts of particles, leading to improved lubrication of the concrete mixtures, compared to incorporating GGBS in the SF concrete mixtures [41, 47].

It is worth noting here that V-funnel times of the ternary binder mixtures with GGBS (OG30S7 and OG30S10) are the highest among all the mixtures with SF, but their T-50_{cm} values are lower than those of the binary SF mixtures (OS7 and OS10). This is because surface friction becomes more dominant when the mixtures flow through the narrow channel of the V-funnel as solid particles are forced to have more contacts and collisions at the narrow space. Therefore, the mixtures with GGBS show larger V-funnel times due to the higher friction of GGBS particles. The effects of friction are smaller in the case of T-50_{cm} as the deformation of the T-50_{cm} test is a free gravitational flow where solid particles are not forced to come into close contact at the narrow space.

3.3.1 Effects of solid volume on T-50_{cm} and V-funnel time

At a high w/b ratio, water content is sufficient for both hydration and lubrication. However, at a low water to binder ratio, water is insufficient for lubrication. Thus, increasing solid volume concentration reduces the occupied water inside the inter-particular voids due to reduced void content and increases the amount of water outside the voids which is effective for lubricating the mixtures. As a result, one of the essential parameters affecting deformability and viscosity is solid volume. Increasing solid volume increases the particle distance and increases the free water for lubrication in the mixtures.

The solid volume vs. T-50$_{cm}$ and solid volume vs. V-funnel time relationships are plotted in Fig. 9. As shown in Fig. 9, T-50$_{cm}$ and V-funnel times of all the tested mixtures correlate well with their solid volumes. The higher the solid volumes, the lower the T-50$_{cm}$ and V-funnel times obtained for the tested HSC mixtures. This indicates that for a fixed w/b ratio, pastes with higher solid volumes of the fine powder will result in lower viscosity. Therefore, the ternary binder mixtures, C-FA-SF, have the lowest viscosity, and so the lowest T-50$_{cm}$ and V- funnel time.

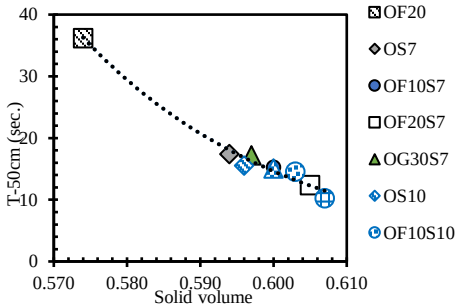

(a) Solid volume vs. T-50$_{cm}$.

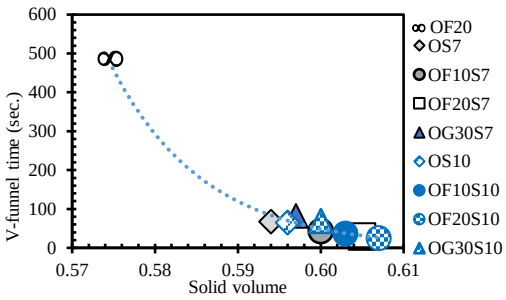

(b) Solid volume vs. V-funnel time.

Fig. 9. Relationship of solid volume vs. T-50$_{cm}$ (a) and solid volume vs. V-funnel time (b) of the tested HSC mixtures.

3.4 Effects of fly ash on compressive strength of HSC mixtures

The effects of fly ash on compressive strength of the tested HSC mixtures at 7 days, 28 days, and 91 days are shown in Fig. 10.

The 7-day compressive strength of the OF20 mixture is the lowest among all the tested mixtures. The ternary binder mixtures incorporating FA (OF10S7, OF10S10, OF20S7, OF20S10) show lower compressive strength than the binary SF mixtures (OS7, OS10), and 7-day compressive strength decreases when increasing FA replacement from 10% to 20%. Nevertheless, with the use of GGBS in the SF mixtures (OG30S7, OG30S10), the values of 7-day compressive strength of the mixtures are slightly higher than those of the SF-only mixtures.

The 28-day compressive strength of the OF20 mixture is still the lowest, whereas that of OS7 is the highest among all the tested HSC mixtures. The 28-day compressive strengths of C–SF–FA mixtures are lower than those of SF binary binder mixtures at the same SF content. However, they are still higher than that of FA binary mixture (OF20). The 28-day compressive strength of HSC mixtures with GGBS are lower than SF binary mixtures, but it is higher than the ternary binder mixtures containing FA. The 28-day compressive strength of all the tested HSC mixtures meets the target compressive strength of 83MPa.

The 91-day compressive strengths of the OG30S7 and OG30S10 mixtures are the highest, followed by OS7, OS10, OF20S7, OF20S10, and OF20 mixtures. The use of only FA as the SCM in the binary binder HSC mixture gives the lowest compressive strength among all the tested HSC mixtures. By incorporating 20% FA or 30% GGBS in SF mixtures, the 91-day compressive strengths of the ternary binder HSC mixtures containing FA are equivalent to those of the SF binary mixtures, while the 91-day compressive strengths of the ternary binder HSC mixtures containing GGBS are higher than those of the SF binary mixtures, when compared at the same SF content.

Since silica fume is typically used in HSC mixtures, to rationally compare the strength performance of all the tested mixtures with the HSC mixtures with only SF as the SCM, the compressive strength results are presented in Fig. 11 in terms of the relative

compressive strength. The relative compressive strength is the percentage of the compressive strength of the considered concrete mixture relative to the compressive strength of the corresponding SF binary mixture (OS7 or OS10), as the reference mixture, at each tested age.

The compressive strength development of each tested HSC mixture depends on the combination of FA, SF, or GGBS in the mixtures. It can be briefly explained in the aspects of the capability of SCMs in terms of packing density and hydration and pozzolanic reactions in the HSC mixtures at different ages.

At an early age, the pozzolanic reaction of SF is the fastest among all SCMs. It highly boosts the strength development because of the effective filler and pozzolanic effects with ultrafine particles [48] and the presence of high crystallized SiO_2 content [49]. As a result, the use of SF in concrete mixtures enhances the early-age compressive strength. On the other hand, FA replacement causes cement dilution, delays cement hydration, has a slow pozzolanic reaction, and does not contribute as much to filler effects as SF. In the case of ternary binders that combine GGBS or FA into SF mixtures, GGBS contributes to the hydration reaction first, then the pozzolanic reaction later, whereas FA contributes only to the pozzolanic reaction [16, 50]. Thus, the 7–day compressive strengths of the C–SF–GGBS mixtures are higher than those of the C–SF–FA mixtures. Although GGBS has a slower reaction than cement, the C–SF–GGBS mixtures show higher 7-day compressive strength than the C–SF mixture. This reveals a significant contribution of the packing density of C–SF–GGBS mixtures, which is higher than that of the C–SF mixture, as shown in Fig. 1. However, the 28-day compressive strengths of SF-only mixtures are higher than those of ternary binder C–SF–FA and C–SF–GGBS mixtures. GGBS and FA have lower reactivity than cement and SF at the first 28 days, as reported by Yu et al. [42], resulting in the lower 28-day compressive strength in ternary binders incorporating FA or GGBS in SF mixtures.

At 91 days, the compressive strengths of the tested HSC mixtures with FA (OF20, OF10S7, OF20S7, OF10S10, OF20S10) increase steadily, significantly, etc. whereas the compressive strengths of HSC binary mixtures containing SF–only (OS7, OS10) do not increase much. Ternary binder C–SF–FA mixtures provide equivalent 91-day compressive strength to SF binary mixtures. On the other hand, the C–SF–GGBS mixtures (OG30S7, OG30S10) have higher compressive strength than all the tested HSC mixtures due to the combined effects of the packing density and hydration reaction of GGBS mixtures during the early stages.

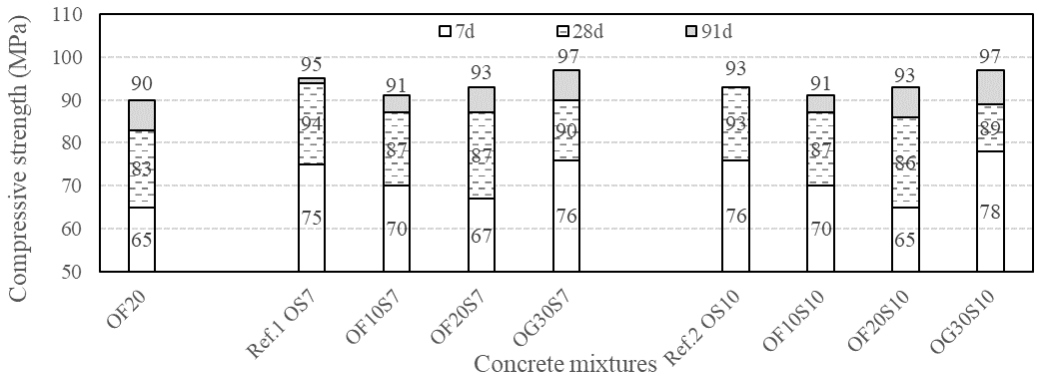

Fig. 10. The influences of binder on compressive strength of tested HSC mixtures.

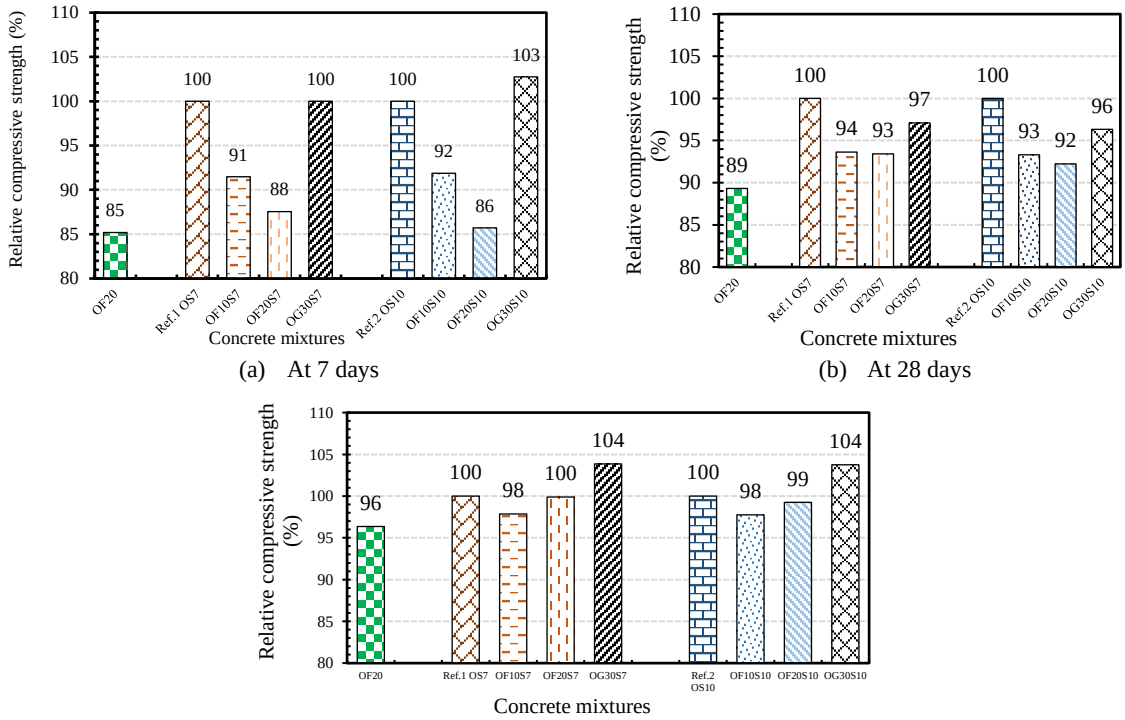

(a) At 7 days

(b) At 28 days

(c) At 91 days

Fig. 11. Relative compressive strength of tested HSC mixtures.

3.5 Effects of fly ash on durability of HSC mixtures

Among the tested HSC mixtures, the mixtures in the group of 7% SF have slightly higher strength than the mixtures in the group of 10% SF. As a result, the group of 7% SF was selected to investigate durability properties, except for the evaluation of autogenous shrinkage where the group of mixtures with 10% SF was additionally tested. The tested durability properties are autogenous shrinkage, semi-adiabatic temperature rise, carbonation resistance, and rapid chloride permeability.

3.5.1 Effects of fly ash on autogenous shrinkage

Fig. 12 demonstrates the results of autogenous shrinkage of the tested HSC mixtures. The binary mixture containing 20% FA (OF20) shows the lowest autogenous shrinkage. When compared to the 7% and 10% SF binary mixtures (OS7 and OS10), incorporating FA into those mixtures reduces autogenous shrinkage. On the other hand, adding 30% GGBS to the SF mixtures increases autogenous shrinkage. FA is known to be effective in reducing autogenous shrinkage of the HSC.

When Portland cement is replaced with FA, GGBS, or SF in HSC, the hydration and pozzolanic characteristics of the materials are altered. The reaction of FA is slow, and it also delays early hydration of cement compared to SF or GGBS. The use of GGBS or SF leads to a tremendous and quick reaction, resulting in large autogenous shrinkage [22, 51]. In addition, in a closed, isothermal cementitious material system, the behavior of autogenous shrinkage in concrete is linked to internal relative humidity in the mixtures [52]. As a result of incorporating FA into HSC mixtures, internal relative humidity in the mixtures decreases slowly due to slow reaction, so self-desiccation and autogenous shrinkage are limited [53].

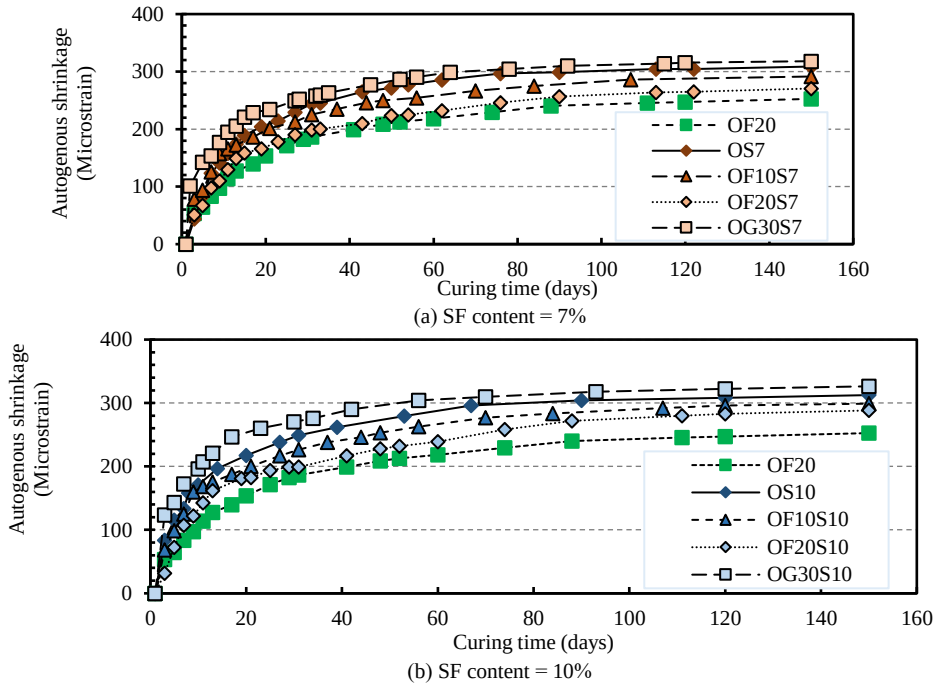

Fig. 12. Autogenous shrinkage of the tested HSC mixtures.

3.5.2 Effects of fly ash on semi-adiabatic temperature rise

Due to the large cement content in the HSC mixture, HSC generates more heat than ordinary concrete. In this study, FA or GGBS is used to partially replace cement, resulting in a lower overall cement content while maintaining the same high strength level. As a result of reducing cement, heat generation in the HSC mixtures is reduced due to less produced hydration heat. Semi-adiabatic temperature rise is used to determine heat generation in the tested HSC mixtures, with the results shown in Fig. 13.

Table 6 summarizes the time to start hydration acceleration, the maximum temperature, and time at maximum temperature obtained from the semi-adiabatic temperature rise results of all the tested mixtures in Fig. 13. It should be noted that the low maximum temperature rise and more delayed time to reach maximum temperature are favorable for mass concrete.

As can be seen from Table 6, the OF20 mixture has the shortest time to start hydration acceleration after concrete casting, followed by OS7, OF20S7, and OG30S7 mixtures. The time to start hydration acceleration (hours) is defined by the intersection of the latest segment of small hydration slope and the first segment of accelerated hydration slope, as shown in Fig. 13. Since the slump flows of the tested HSC mixtures containing FA, GGBS, and SF were controlled at 65 ± 1cm, they have different superplasticizer dosages, especially dosage relative to cement (SP/C) in a ratio by weight. The SP/C ratios of OF20, OS7, OF20S7, and OG30S7 HSC mixtures are 0.016, 0.02, 0.022, and 0.027, respectively. It is anticipated that a greater SP/C ratio means a thicker layer of SP covering the cement particles, resulting in more retarded hydration, as can be seen in Fig. 14. Thus, the fly ash-only mixture (OF20) started accelerating hydration earlier than the silica fume-only mixture (OS7), and the OF20S7 mixture began accelerating hydration earlier than the OG30S7 mixture. This observation on the effect of SP on hydration acceleration time was also reported by Lee et al. [54].

After retarding hydration time, the acceleration of the hydration reaction of HSC

mixtures is initiated, which greatly generates heat leading to a change of slopes of the curves and finally reaching maximum temperature. As shown in Table 6, the maximum temperature of the OF20 mixture (73.3ºC) is slightly higher than that of the OS7 mixture (72.7ºC). However, incorporating FA or GGBS in the SF mixtures to obtain OF20S7, OG30S7 mixtures reduces temperature compared to the OS7 mixture. The maximum temperature of the 20% FA (OF20S7) and 30% GGBS (OG30S7) mixtures are 67.6ºC and 67.8ºC, respectively. Although the 30%GGBS mixture has higher cement replacement than the 20% FA, the maximum temperature rises of the OG30S7 and OF20S7 mixtures are equivalent. From the results, it can be realized that the ternary binder mixtures (OF20S7, OG30S7) have lower rates of heat and lower maximum temperature than the binary binder mixtures (OF20, OS7). Moreover, the time at a maximum temperature of the OS7 mixture is the shortest (19.3 hours), followed by OG30S7 (21.6 hours), OF20S7 (21.7 hours), and OF20 (22.7 hours). The SF binary mixture delivers the shortest time at maximum temperature.

Several characteristics of the SCMs should be addressed to fully comprehend these phenomena. Heat generation is related to the rate of hydration and the pozzolanic reaction of the tested HSC mixtures. The fineness of SF is very high. It also has a high content of reactive SiO_2. So, SF is very reactive with $Ca(OH)_2$ during cement hydration [48, 55]. As a result, the binary HSC mixture with SF has the fast rate of reaction. On the other hand, the w/b ratio is relatively low, leading to restricted cement hydration. Thus, the maximum temperature values of the OS7 mixture and OF20 mixture are not much different. This finding is expected to be associated with various factors, so further studies are necessary to determine clearer reasons.

The ternary binder mixtures incorporating GGBS, and FA (OG30S7 and OF20S7) have lower maximum temperature due to lower proportions of cement for hydration reaction compared to the binary binder mixtures (OS7, OF20). Using 20% FA as a cement replacement in the OF20S7 mixture results in equivalent maximum temperature to using 30% GGBS in the OG30S7 mixture. This is because GGBS also contributes to hydration reaction. However, the FA mixture (OF20S7) shows longer time at maximum temperature than the GGBS mixture (OG3S7) because FA has a slower reaction than GGBS [42]. For more support, Qiang et al. [56] reported that with the same proportion of cement replacement, the early reaction of GGBS is higher than FA because GGBS also has hydration reaction, while the report by Choktaweekarn et al. [57] stated that the use of FA reduces cement hydration at an early age because it delays cement hydration at an early age.

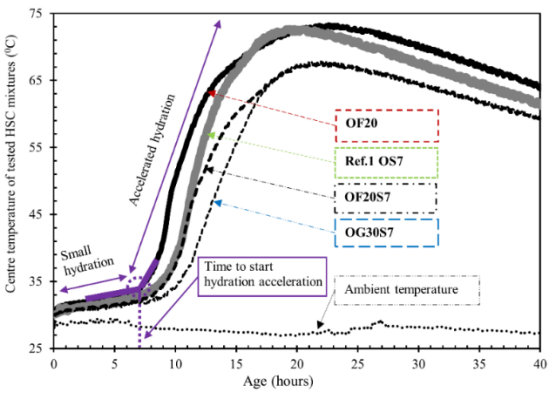

Fig. 13. Results of semi-adiabatic temperature rises of tested HSC mixtures.

Table 6. Time to start hydration acceleration, maximum temperature, and time at maximum temperature of tested the HSC mixtures.

HSC mixtures	Time to start hydration acceleration (hours)	Maximum temperature (˚C)	Time at maximum temperature (hours)
OF20	7.6	73.3	22.7
Ref.1 OS7	8.9	72.7	19.3
OF20S7	9.3	67.6	21.7
OG30S7	10.5	67.8	21.6

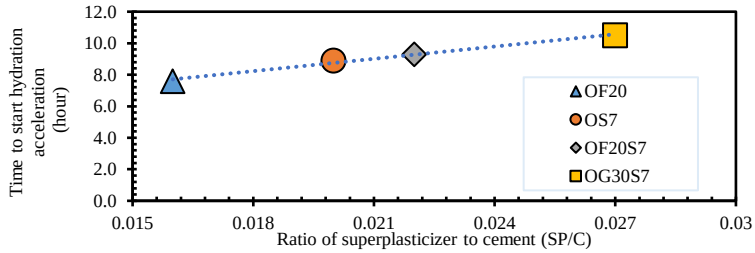

Fig. 14. Relationship between time to start accelerating hydration and ratio of superplasticizer to cement content (SP/C).

3.5.3 Effects of fly ash on carbonation resistance

All the tested HSC mixtures demonstrate no carbonation depth, as shown in Fig. 15. Though FA is known to reduce alkalinity in the concrete, resulting in lower carbonation resistance, at this level of low w/b, the HSC mixtures have extremely low porosity, causing all tested mixtures to show zero carbonation depth throughout the test period.

3.5.4 Effects of fly ash on rapid chloride permeability

Fig. 16 shows the chloride permeability results tested at the specimen ages of 28 and 91 days using the RCPT method. The OF20 mixture shows very low chloride permeability at 28 and 91 days according to ASTM C1202. However, the other HSC mixtures possess negligible chloride permeability at the ages of 28 and 91 days [37]. The results of chloride permeability are correlated with the pore structures of the tested mixtures, as explained in the following section.

(a) (b) (c) (d)

Fig. 15. Carbonation depths of the tested specimens: (a) OF20, (b) Ref.1 OS7, (a) OF20S7, (d) OG30S7.

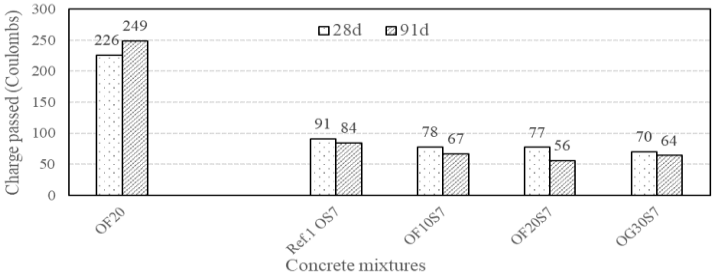

Fig. 16. Rapid chloride permeability of tested HSC mixtures.

3.6 Relationship between pore structures and chloride permeability of the HSC mixtures

3.6.1 Pore structure of mortar mixtures by MIP

The results of the MIP are used in this study to derive the pore structure parameters of the tested mortar mixtures. The results of cumulative pore volume (mL/g) of the tested mortar mixtures are shown in Fig. 17.

The pore size structures were classified into gel pores (2-10nm), capillary pores (10-50nm), and macrospores (>50nm), according to Aligizaki et al. [58]. Fig. 18a depicts the cumulative pore volumes of the tested mixtures according to this pore size classification. Fig. 18b shows the calculated total pore volumes and average pore diameters of the tested mixtures, considering pores that are larger than 10 nm (capillary and macropores).

The OF20 mixture has the highest total pore volume, followed by the OF20S7, OS7, and OG30S7 mixtures. For average pore diameter, OF20 has the highest average pore diameter, followed by OS7, OG30S7, and OF20S7 mixtures. It can be concluded that the inclusion of GGBS or FA to obtain ternary binder HSC mixtures can refine the pore structure of the mixtures as the average pore size becomes smaller.

Anwar et al. [59] also reported that cementitious blends as ternary binders of C–FA–SF result in better pore structure than binary binder C–SF and OPC–only mixtures. It should be noted here that the results of MIP shown in Fig. 17 were obtained from specimens at the age of 28 days. It is expected that at 91 days of age, the total pore volume of OF20S7 may be lower than that of the OG30S7.

3.6.2 Relationship between pore structures and chloride permeability of the HSC mixtures

The pore structure is the primary factor that influences the chloride permeability of concrete. The average pore diameter and volume of pores bigger than 10nm (the macrospores and capillary pores) are known to associate with the chloride permeability of concrete, whereas gel pores have little influence. Fig. 19 shows the correlation between rapid chloride permeability (coulombs) and pore characteristics (average pore size and total pore volume of pores larger than 10nm) of the tested HSC mixtures.

The total volume of pores greater than 10nm and the average pore size have good correlations with the charge passed values. The charge passed of the tested HSC mixture increases as the average pore size and the volume of pores larger than 10nm increase. Both have been reported to be necessary for evaluating the diffusion coefficient of Cl^- in concrete [60].

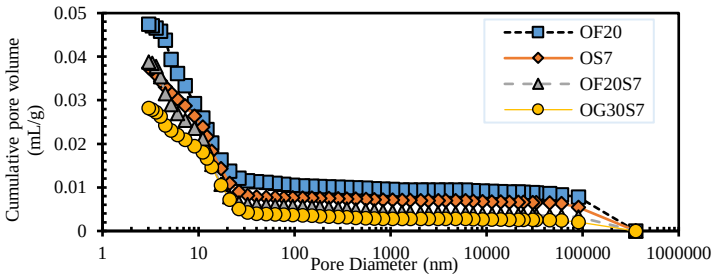

Fig. 17. Cumulative pore volume (mL/g).

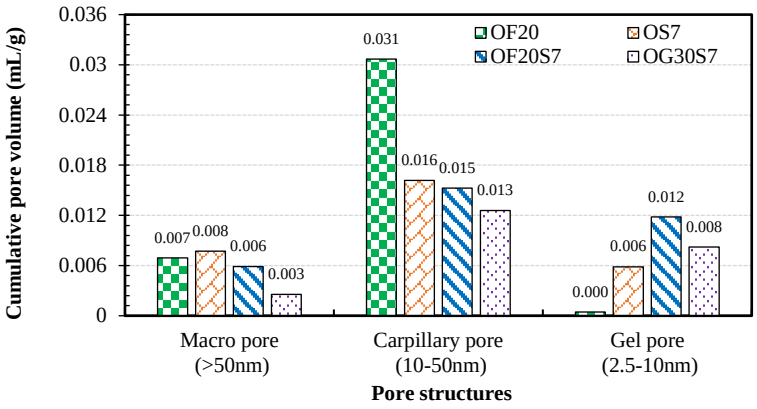

(a) Classified pore volume based on pore types

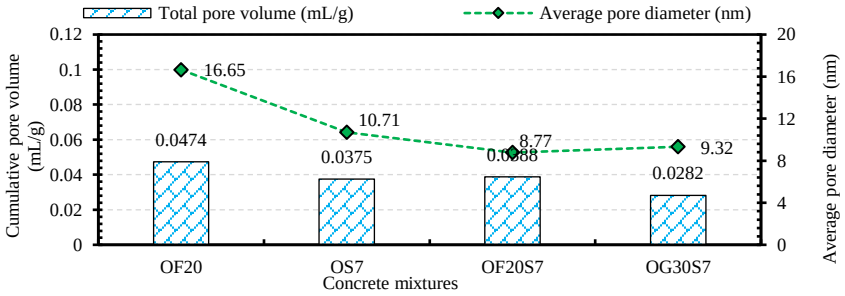

(b) Cumulative pore volume and average pore diameter

Fig. 18. Pore structures of the tested mortar mixtures at the age of 28 days.

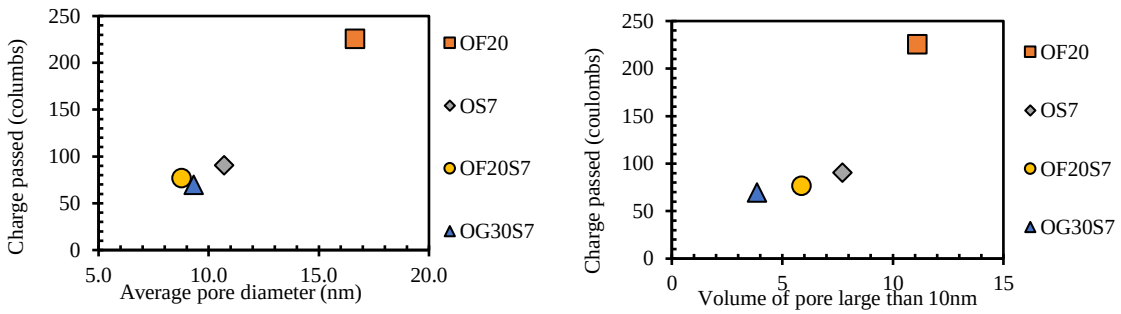

(a) RCPT and average pore diameter of pores larger than 10nm

(b) RCPT and volume of pores larger than 10nm

Fig. 19. Relationship between rapid chloride permeability (RCPT) and pore structures of the tested HSC mixtures at 28 days of age.

3.7 Cost-effectiveness of HSC mixtures

As the costs of materials vary depending on regions, this section provides only a rough comparison of the unit costs of the HSC mixtures based on the tested mix proportions. The unit costs of raw materials were obtained from Singapore, Thailand, and Vietnam markets, which were average data from several local suppliers, as presented in Table 7. As shown in Table 7, in all 3 countries, the unit cost of FA is lower than GGBS or SF.

The unit costs of the tested HSC mixtures were calculated to analyze the cost-effectiveness, as presented in Fig. 20. The results show that incorporating FA and GGBS in HSC mixtures gives lower costs than the

reference mixtures (OS7 and OS10). The unit costs of all tested HSC mixtures containing FA are lower than those of the mixtures without FA. Thus, the utilization of FA helps to reduce the mixture costs.

Table 7. Unit prices of HSC mixture components.

Types	Components	Prices of the studied market (USD/ton)		
		Singapore[1)]	Thailand[2)]	Vietnam[3)]
Binders	Cement (OPC)	80	60	54
	Fly ash (FA)	65	40	25
	Ground granulated blast furnace slag (GGBS)	73	60	41
	Silica fume (SF)	300	480	294
High range water reducer	Superplasticizer (SP)	2200	990	1513
Aggregates	Coarse aggregate	20	7	9
	Fine aggregate	20	5	7

Note: 1) Sources from Taiheiyo Cement Corporation, Singapore. 2) Sources from SCG Co, Ltd., Siam Cement City Group., and Wanna et al. [61]. 3) Sources from Vicem Ha Tien, Vietgo Company Limited, FiCo Tay Ninh Cement, and Tan Thuy mineral Joint Stock Company

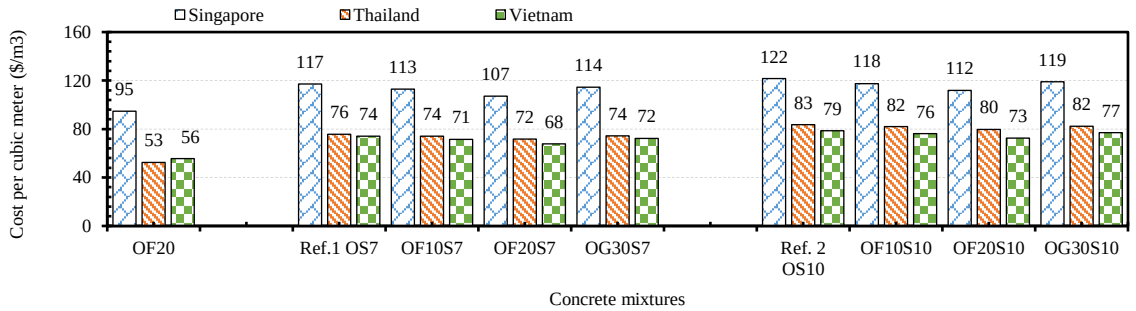

Fig. 20. Unit cost comparisons of the tested HSC mixtures

3.8 Relative overall performance of HSC mixtures

The overall performances of HSC mixtures are compared using relative performance weight ratios and a radar chart for evaluation. Relative overall performances of the tested mixtures, including FA–only (OF20), fly ash and silica fume (OF20S7) mixture, GGBS and SF (OG30S7) mixture are compared with the 7%SF HSC mixture (OS7) as the reference mixture, as summarized in Fig. 21. It is noted that only the series of 7% SF mixtures is used to compare the relative overall performances as the series of the 10%SF mixtures also gives the same trend.

The T-50_{cm}, V-funnel, autogenous shrinkage (91 days), early-age strength (28 days), later-age strength (91 days), carbonation depth, chloride permeability by RCPT, maximum semi-adiabatic temperature rise, and cost-effectiveness of the tested HSC mixtures are used to calculate the relative performance values of the tested HSC mixtures. To calculate the relative performance values, the SF reference mixture (OS7) is used as the control mixture, with a relative performance value of 1.0 (100%). Relative performance values of the other tested HSC mixtures are calculated based on the performance of the OS7 mixture as the reference. When the value is 1.0 (100%), the mixture performs similarly to the OS7 mixture. When the value is lower than 1.0 (100%), the mixture performs poorer, but when the value is greater than 1.0 (100%), the mixture performs better than the reference OS7 mixture. The calculation follows Eq. (3.1):

$$R_{HSC} = 1.0 \pm \frac{|P_{HSC} - P_{OS7}|}{P_{OS7}} \times 100, \qquad (3.1)$$

where R_{HSC} is the relative performance value of a considered HSC mixture, P_{HSC} is the performance of the considered HSC mixture.

P_{OS7} is the performance of the reference mixture (OS7).

It is noted that in Eq. (3.1), if a property of the considered HSC mixture is better than that of the reference OS7 mixture, the 2nd term on the right side of the equation after the "1.0" is assigned the plus sign, whereas minus is assigned if the property is worse than that of the reference OS7 mixture.

The calculated relative performance values are used to plot the radar chart as shown in Fig. 21. The ternary binder HSC mixture with fly ash and silica fume (OF20S7) performs better than the other mixtures (OF20, OS7, OG30S7). Almost all relative performance values of OF20S7 are at the most outside of the radar chart. Therefore, it can be concluded that the incorporation of FA in SF mixtures can enhance performances of the SF HSC mixture, especially in the aspects of viscosity, autogenous shrinkage, heat generation, as well as cost-effectiveness while having equivalent strength at 91 days.

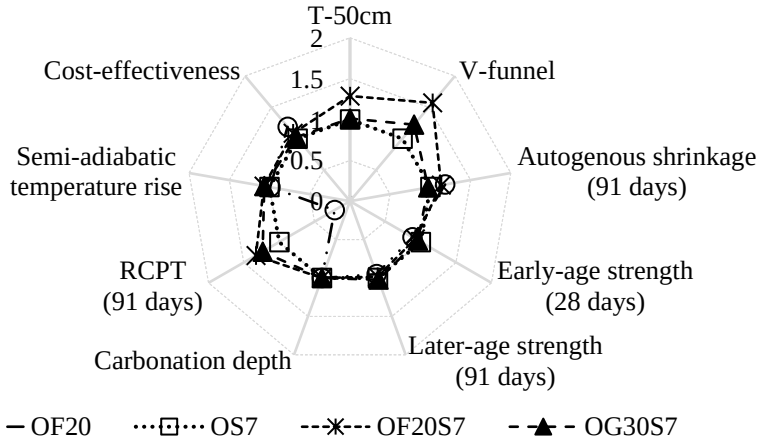

Fig. 21. Relative performances of the tested HSC mixtures compared to the reference OS7 mixture.

4. Conclusion

The studies of binary and ternary binders containing 10% or 20% fly ash, 7% or 10% silica fume, and 30% ground granulated blast furnace slag on viscosity, autogenous shrinkage, temperature rise, compressive strength, carbonation, and RCP properties of HSC mixtures with a target slump flow and compressive strength of 65±1cm. and 83MPa, respectively, were conducted. The following conclusions are obtained from the test results:

The use of FA is significantly effective in enhancing slump flow while reducing the superplasticizer dosage. In terms of the ternary binder mixtures with SF, FA is better than GGBS. FA can significantly reduce the viscosity of HSC mixtures.

1) Compared to the reference silica fume binary binder mixtures, the ternary binder HSC mixtures containing FA have lower autogenous shrinkage and maximum temperature rise. The maximum temperature is not significantly different between the ternary binder C–SF–FA and C–SF–GGBS mixtures.
2) Although the use of FA in HSC mixtures with SF reduces early-age compressive strength, it improves compressive strength at a later age. The mixtures of HSC containing 20% FA and 7% or 10% SF show slightly lower 7-day and 28-day compressive strengths than the SF-only mixtures, but their 91-day compressive strengths are equivalent to those of the SF-

only mixtures. The use of GGBS in SF mixtures gives higher compressive strength compared to the binary SF mixtures and the ternary binder mixture with SF and FA.

3) The use of FA in SF mixtures results in low chloride permeability due to improved pore structure.
4) All the tested HSC mixtures show no carbonation depth due to very low w/b, leading to very dense pore structures.
5) The tested RCP values have good correlations with total volume of pores and average pore diameter obtained from MIP. The ternary binder HSC mixtures containing FA and GGBS have a denser pore structure than the binary binder containing only FA or SF, resulting in lower rapid chloride permeability.
6) The use of FA as a partial cement replacement in SF HSC mixtures reduces viscosity, autogenous shrinkage, hydration heat, chloride permeability while maintaining the compressive strength performance compared to the SF binary mixture. Furthermore, employing FA in HSC concrete mixtures reveals cost-effectiveness.

Conflict of Interests

The authors declare that there are no conflicts of interest regarding the publication of this article.

Acknowledgements

The first author would like to thank the "Excellent Foreign Students (EFS) scholarship program of Sirindhorn International Institute of Technology (SIIT), Thammasat University. This research was supported by Taiheiyo cement Corporation-Japan, and Center of Excellence in Material Science, Construction and Maintenance Technology, Thammasat University, and the Chair Professor Program (P-19-52302), the National Science and Technology Development Agency (NSTDA).

References

[1] Shannag, M.J. High strength concrete containing natural pozzolan and silica fume. Cement and Concrete Composites. 2000;22(6):399-406.

[2] ACI Committee 363. High-Strength Concrete (ACI 363R). ACI Symposium Publication. 2005.

[3] Skalny, J., Roberts, L.R. High-Strength Concrete. Annual Review of Materials Science. 1987;7(1):35-56.

[4] Vejmelková, E, Koňáková, D, Čáchová, M, Záleská, M, Svora, P, Keppert, M, Rovnanikova, P, Černý, R. High-strength concrete based on ternary binder with high pozzolan content. Structural Concrete. 2018;19(5): 1258-67.

[5] Scrivener, KL, Kirkpatrick, RJ. Innovation in use and research on cementitious material. Cement and Concrete Research. 2008;38(2):128-36.

[6] Park, JH, Edraki, M, Mulligan, D, Jang, HS. The application of coal combustion by-products in mine site rehabilitation. Journal of Cleaner Production. 2014;84:761-72.

[7] Hasanbeigi, A, Price, L, Lin, E. Emerging energy-efficiency and CO2 emission-reduction technologies for cement and concrete production: A technical review. Renewable and Sustainable Energy Reviews. 2012;16(8):6220-38.

[8] Bijen, J. Benefits of slag and fly ash. Construction and Building Materials. 1996;10(5):309-14.

[9] Naik, TR. Sustainability of Concrete Construction. Practice Periodical on Structural Design and Construction. 2008;13(2):98-103.

[10] Caldarone, MA. High-Strength Concrete: A Practical Guide (1st ed.). London, 2014. 272.

[11] Holland Terence, C. Silica Fume User's Manual. 2005. Lovettsville.

[12] Wu, M, Li, C, Yao, W. Gel/space ratio evolution in ternary composite system consisting of Portland cement, silica fume, and fly Ash. 2017. Materials. 10(1).

[13] Bhanja, S, Sengupta, B. Optimum Silica fume content and its mode of action on concrete. ACI Materials Journal. 2003. 100(5).

[14] Mala, K, Mullick, AK, Jain, KK, Singh, PK. Effect of relative levels of mineral admixtures on strength of concrete with ternary cement blend. International Journal of Concrete Structures and Materials. 2013;7(3):239-49.

[15] Johari, MAM., Brooks, JJ, Kabir, S, Rivard, P. Influence of supplementary cementitious materials on engineering properties of high strength concrete. Construction and Building Materials. 2011;25(5):2639-48.

[16] Regourd, M, Thomassin, JH, Baillif, P, Touray, J.C. Blast-furnace slag hydration. Surface analysis," Cement and Concrete Research. 1983;13(4):549-56.

[17] Yalçınkaya, Ç, Çopuroğlu, O. Hydration heat, strength and microstructure characteristics of UHPC containing blast furnace slag. Journal of Building Engineering. 2021;34:101915.

[18] Kovács, R. Effect of the hydration products on the properties of fly-ash cements. Cement and Concrete Research. 1975;5(1):73-82.

[19] Fajun, W, Grutzeck, MW, Roy, DM. The retarding effects of fly ash upon the hydration of cement pastes: The first 24 hours. Cement and Concrete Research. 1985;15(1): 174-84.

[20] ACI committee 211, "Guide for selecting proportions for High-strength concrete using Portland cement and other cementitious materials," ACI 211.4R-08, 2008.

[21] Antiohos, S, Tsimas, S. Activation of fly ash cementitious systems in the presence of quicklime: Part I. Compressive strength and pozzolanic reaction rate. Cement and Concrete Research. 2004;34(5):769-79.

[22] Yoo, DY, Min, KH, Lee, JH, Yoon, YS. Autogenous shrinkage of concrete with design strength 60–120 N/mm2. Magazine of Concrete Research. 2011;63(10):751-61.

[23] Nath, P, Sarker, PK, Biswas, WK. Effect of fly ash on the service life, carbon footprint and embodied energy of high strength concrete in the marine environment. Energy and Buildings. 2018;158:1694-702.

[24] Lee, KM, Lee, HK, Lee, SH, Kim, GY. Autogenous shrinkage of concrete containing granulated blast-furnace slag. Cement and Concrete Research. 2006;36(7):1279-85.

[25] Erdem, TK, Kırca, Ö. Use of binary and ternary blends in high strength concrete. Construction and Building Materials. 22(7):1477-83.

[26] Anwar, M, Emarah, DA. Resistance of concrete containing ternary cementitious blends to chloride attack and carbonation. Journal of Materials Research and Technology. 2020;9(3):3198-207.

[27] ASTM C150/C150M-20. Standard Specification for Portland Cement. ASTM International. West Conshohocken. PA. 2020.

[28] ASTM C494/C494M-19. Standard Specification for Chemical Admixtures for Concrete. ASTM International. West Conshohocken. PA. 2019.

[29] ASTM C33 / C33M-08. Standard Specification for Concrete Aggregates. ASTM International. West Conshohocken. PA. 2008.

[30] Wong, HHC, Kwan, AKH. Packing density of cementitious materials: part 1—measurement using a wet packing method. Materials and Structures. 2008;41(4):689-701.

[31] Qiu, J, Guo, Z, Yang, L, Jiang, H, Zhao, Y. Effects of packing density and water film thickness on the fluidity behaviour of cemented paste backfill. Powder Technology. 2020;359:27-35.

[32] ASTM C1611 / C1611M-18. Standard Test Method for Slump Flow of Self-Consolidating Concrete. ASTM International. West Conshohocken. PA. 2018.

[33] EN 12350-9. Testing fresh concrete—Part 9: Self-compacing concrete—V-funnel test. 2010.

[34] ASTM C39/C39M - 20. Standard Test Method for Compressive Strength of Cylindrical Concrete Specimens. ASTM International. West Conshohocken. PA.

[35] ASTM C157 / C157M-17. Standard Test Method for Length Change of Hardened Hydraulic-Cement Mortar and Concrete. ASTM International. West Conshohocken. PA, 2017.

[36] RILEM TC 56-MHM. CPC-18 Measurement of hardened concrete carbonation depth. RILEM Publications SARL. 1988;21(126):453-5.

[37] ASTM C1202-19. Standard Test Method for Electrical Indication of Concrete's Ability to Resist Chloride Ion Penetration. ASTM International. West Conshohocken. PA. 2019.

[38] Mehdipour, I, Khayat, KH. Effect of supplementary cementitious material content and binder dispersion on packing density and compressive strength of sustainable cement paste. ACI Materials Journal. 2016;113(3):51688704.

[39] Mehdipour, I, Khayat, KH. Effect of particle-size distribution and specific surface area of different binder systems on packing density and flow characteristics of cement paste. Cement and Concrete Composites. 2017;78:120-31.

[40] Bagheri, AR, Zanganeh, H, Moalemi, MM. Mechanical and durability properties of ternary concretes containing silica fume and low reactivity blast furnace slag. Cement and Concrete Composites. 2012;34(5):663-70.

[41] Chen, B, Liu, J. Experimental application of mineral admixtures in lightweight concrete with high strength and workability. Construction and Building Materials. 2008;22(6):1108-13.

[42] Yu, R, Spiesz, P, Brouwers, HJH. Development of an eco-friendly ultra-high performance concrete (UHPC) with efficient cement and mineral admixtures uses. Cement and Concrete Composites. 2015;55:383-94.

[43] EFNARC. Specification and Guidelines for Self-Compacting Concrete. The European Federation of Specialist Construction Chemicals and Concrete Systems. 2005.

[44] Elrahman, MA, Hillemeier, B. Combined effect of fine fly ash and packing density on the properties of high performance concrete: An experimental approach. Construction and Building Materials. 2014;58:225-33.

[45] Chen, JJ, Ng, PL, Chu, SH, Guan, GX, Kwan, AKH. Ternary blending with metakaolin and silica fume to improve packing density and performance of binder paste. Construction and Building Materials. 2020;252: 119031.

[46] Khunthongkeaw, J, Tangtermsirikul, S. Vibration consistency prediction model for roller-compacted concrete (RCC). ACI Materials Journal. 2003;100(1):12457.

[47] Zou, RP, Yu, AB. Evaluation of the packing characteristics of mono-sized non-spherical particles. Powder Technology. 1996; 88(1):71-9.

[48] Rahhal, V, Bonavetti, V, Trusilewicz, L, Pedrajas, C, Talero, R. Role of the filler on Portland cement hydration at early ages. Construction and Building Materials. 2012:27(1):82-90.

[49] Kadri, EH, Aggoun, S, De Schutter, G, Ezziane, K. Combined effect of chemical nature and fineness of mineral powders on Portland cement hydration. Materials and Structures. 2010;43(5):665-73.

[50] Wu, X, Jiang, W, Roy, DM. Early activation and properties of slag cement. Cement and Concrete Research. 1990;20(6):961-74.

[51] Zhang, MH, Tam, CT, Leow, MP. Effect of water-to-cementitious materials ratio and silica fume on the autogenous shrinkage of concrete. Cement and Concrete Research. 2003;33(10):1687-94.

[52] Jiang, C, Yang, Y, Wang, Y, Zhou, Y, Ma, C. Autogenous shrinkage of high performance concrete containing mineral admixtures under different curing temperatures. Construction and Building Materials. 2014;61:260-9.

[53] Zhao, Y, Gong, J, Zhao, S. Experimental study on shrinkage of HPC containing fly ash and ground granulated blast-furnace slag. Construction and Building Materials. 2017;155:145-53.

[54] Lee, JH, Yoon, YS. The effects of cementitious materials on the mechanical and durability performance of high-strength concrete. KSCE Journal of Civil Engineering. 2015;19(5):1396-404.

[55] Oey, T, Kumar, A., Bullard, JW, Neithalath, N., Sant, G. The filler effect: The influence of filler content and surface area on cementitious reaction rates. Journal of the American Ceramic Society. 2013;96(6):1978-90

[56] Qiang, W, Mengxiao, S, Dengquan, W. Contributions of fly ash and ground granulated blast-furnace slag to the early hydration heat of composite binder at different curing temperatures. Advances in Cement Research. 2016;28(5):320-7.

[57] Tangtermsirikul, S, Choktaweekarn, P. A model for predicting the coefficient of thermal expansion of cementitious paste. 2009;35:57.

[58] Aligizaki, KK, "Pore Structure of Cement-Based Materials: Testing, Interpretation and Requirements (1st ed.). CRC Press. https://doi.org/10.1201/9781482271959.

[59] Anwar, M, Emarah, DA. Pore structure of concrete containing ternary cementitious blends. Results in Materials. 2019;1: 100019.

[60] Sumranwanich, T, Tangtermsirikul, S. A model for predicting time-dependent chloride binding capacity of cement-fly ash cementitious system. Materials and Structures. 2004:37(6):387.

[61] Wanna, S, Saengsoy, W, Toochinda, P, Tangtermsirikul, S. Effects of sand powder on sulfuric acid resistance, compressive strength, cost benefits, and CO2 reduction of high CaO fly ash concrete. Advances in Materials Science and Engineering. 2020. p. 3284975.